Separation Science and Technology
Publication details, including instructions for authors and subscription information:
http://www.informaworld.com/smpp/title~content=t713708471

Propane/Propylene Separation by Simulated Moving Bed II. Measurement and Prediction of Binary Adsorption Equilibria of Propane, Propylene, Isobutane, and 1-Butene on 13X Zeolite

Nabil Lamia[a][b][c]; Miguel A. Granato[a][b]; Pedro SÁ Gomes[a][b]; Carlos A. Grande[a][b]; Luc Wolff[c]; Philibert Leflaive[c]; Damien Leinekugel-le-Cocq[c]; Alírio E. Rodrigues[a][b]
[a] Laboratory of Separation and Reaction Engineering, Associate Laboratory LSRE/LCM, Porto, Portugal [b] Faculty of Engineering, University of Porto, Porto, Portugal [c] Institut Français du Pétrole, IFP-Lyon, Process Design and Modeling Division, Rond Point de l'échangeur de Solaize, Solaize, France

To cite this Article Lamia, Nabil , Granato, Miguel A. , SÁ Gomes, Pedro , Grande, Carlos A. , Wolff, Luc , Leflaive, Philibert , Leinekugel-le-Cocq, Damien and Rodrigues, Alírio E.(2009) 'Propane/Propylene Separation by Simulated Moving Bed II. Measurement and Prediction of Binary Adsorption Equilibria of Propane, Propylene, Isobutane, and 1-Butene on 13X Zeolite', Separation Science and Technology, 44: 7, 1485 — 1509

To link to this Article: DOI: 10.1080/01496390902775935

URL: http://dx.doi.org/10.1080/01496390902775935

Separation Science and Technology, 44: 1485–1509, 2009

ISSN: 0149-6395 print/1520-5754 online
DOI: 10.1080/01496390902775935

Propane/Propylene Separation by Simulated Moving Bed II. Measurement and Prediction of Binary Adsorption Equilibria of Propane, Propylene, Isobutane, and 1-Butene on 13X Zeolite

**Nabil Lamia,[1,2] Miguel A. Granato,[1] Pedro SÁ Gomes,[1]
Carlos A. Grande,[1] Luc Wolff,[2] Philibert Leflaive,[2]
Damien Leinekugel-le-Cocq,[2] and Alírio E. Rodrigues[1]**
[1]Laboratory of Separation and Reaction Engineering,
Associate Laboratory LSRE/LCM; Department of Chemical Engineering,
Faculty of Engineering, University of Porto, Porto, Portugal
[2]Institut Français du Pétrole, IFP-Lyon, Process Design and Modeling
Division, Rond Point de l'échangeur de Solaize, Solaize, France

Abstract: The design of a simulated moving bed (SMB) process relies on valid thermodynamic predictions of multicomponent adsorption built up from accurate binary adsorption equilibrium data. Experimental adsorption equilibria of binary mixtures constituted by propane, propylene, isobutane and 1-butene on 13X zeolite were determined using breakthrough experiments at 373 K and 150 kPa. In addition, these binary adsorption experiments allow to confirm the choice of isobutane as an interesting desorbent for the separation of propane-propylene by SMB, since it has an intermediate selectivity between the two species to separate. Various prediction models are available in the literature but only a few of them have both physical and thermodynamical consistency. The ideal adsorbed solution theory (IAST), the thermodynamically consistent extended Toth model (TCET), and the physically-consistent extended Toth isotherm (PCET) were used to predict binary adsorption equilibria from pure component adsorption isotherms

Received 9 October 2008; accepted 20 December 2008.

Address correspondence to Alírio E. Rodrigues, Laboratory of Separation and Reaction Engineering, Associate Laboratory LSRE/LCM; Department of Chemical Engineering, Faculty of Engineering, University of Porto, Rua Dr. Roberto Frias s/n, Porto 4200-465, Portugal. E-mail: arodrig@fe.up.pt

parameters. The PCET model was found suitable for representing the adsorption equilibrium of the different hydrocarbon mixtures with a reasonably good accuracy.

Keywords: 1-butene, 13X zeolite, binary adsorption equilibrium, breakthrough experiment, extended Toth model, IAST, isobutane, olefin, propane, propene, propylene, separation, simulated moving bed, SMB

INTRODUCTION

The separation of propane-propylene mixture is one of the most important operations in the petrochemical industry. Such mixture usually results from steam cracking and fluid catalytic cracking of heavy petroleum fractions. Currently, the separation of this mixture is carried out by distillation, which is highly energy-intensive due to the small difference in relative volatility between the two components (1). Distillation columns are often up to 100 meter tall and typically contain over 150 trays in order to achieve polymer-grade propylene (purity of $>$ 99.5%). With reflux ratios greater than 10, a large quantity of energy is required for the distillation process (2). The high capital and operating costs of the existing practiced process provides an incentive for the development of alternative separation methods (3,4). One of the most promising alternatives is the adsorption-based separation (5,6) and notably cyclic adsorption processes such as pressure or vacuum swing adsorption (PSA/VSA) technologies (7–11). More recently Rodrigues et al. (12) have reported that an effective separation of this mixture can also be achieved by another cyclic adsorption scheme, namely the simulated moving bed (SMB) process. The principle of this process is to simulate a continuous countercurrent flow of the fluid and of the solid adsorbent by a synchronous port shifting of the different inlets and outlets in a multicolumn unit (13,14). Furthermore, one should notice that the main difference with PSA and VSA processes is the introduction of a high-performance desorbent to regenerate the solid adsorbent. The choice of this desorbent in combination with an adequate adsorbent is therefore particularly important since it is a key element of any SMB process. In previous works, two interesting adsorbent-desorbent systems have been identified: 13X zeolite/isobutane and 13X zeolite/1-butene (15,16).

Besides the identification of a pertinent adsorbent-desorbent couple, the development, design, and operation of this kind of process mainly require the determination of mixture equilibria, i.e., coadsorption isotherms rather than pure component isotherms (17). In fact, a few competitive adsorption data, measured using the mixture to be separated and the potential desorbent, are usually sufficient to set the operating conditions of an SMB (18).

A variety of experimental techniques can be considered for binary adsorption data determination (19). The major ones are static methods and more precisely gravimetric and volumetric techniques or a combination of the two (20–21). However, in this work a dynamic method on a fixed bed adsorption column is employed since in the industrial practice the operation of a SMB process comes close to the experimental procedure used in breakthrough experiments. In addition, this technique allows an exact control of the binary gas phase composition at constant temperature and pressure.

Nevertheless, although the acquisition of experimental binary adsorption data is crucial, it is almost impossible to cover experimentally a wide range of temperature, pressure, and composition conditions. As a consequence of this limitation, several adsorption models, such as the ideal adsorbed solution theory (IAST) (22) or extended Langmuir-type models (23) have been developed to predict binary adsorption equilibrium. Those predictions have the advantage of being only based on single component isotherms and it is often found that the prediction accuracy is perfectly acceptable for rigorous engineering design of cyclic adsorption processes. But most of them do not take into account the physical structure of the adsorbent so their validity is just limited to thermodynamic considerations. For this reason we have extended the so-called Toth model (24) by introducing a physical constraint, i.e., taking into account the 13X zeolite cage dimension and the size of the different adsorbates.

Thus, the main objective of the current study is to provide multicomponent adsorption equilibrium data of different binary systems comprising propane, propylene, isobutane, and 1-butene on 13X zeolite via breakthrough experiments at constant pressure and temperature. Results obtained are then compared with three predictive models based on single-component adsorption isotherms: ideal adsorbed solution theory of Myers and Prausnitz (22), the thermodynamically consistent extended Toth isotherm (TCET) and the physically consistent extended Toth model (PCET).

EXPERIMENTAL SECTION

Adsorbent and Adsorbates

The adsorbent used in this study is a commercial 13X zeolite manufactured by CECA (France) in extrudate form. Some representative properties of the adsorbent are reported in Table 1. The average crystal

Table 1. Physical properties of 13X zeolite

Property	Value
Extrudate radius R_p	0.8 mm
Extrudate length l_p	6.0 mm
Crystal radius r_c	1.0 μm
Water capacity $wt.$	20 %
Pellet density ρ_p	1357 kg.m^{-3}
Pellet porosity ε_p	0.395

size of the sample was obtained by scanning electron microscopy (SEM). The 13X zeolite pore structure consists of sodalite cages interconnected in such a way that 15 Å diameter supercages are accessible through 7.4 Å diameter windows in a tetrahedral arrangement. Due to the presence of nonframework sodium ions, 13X zeolites provides a heterogeneous environment for polar molecules. The propane, propylene, isobutane, and 1-butene used in this work were research-grade pure components, provided by Air Liquide (France). The purity of the sorbate gases was N35 for propane (>99.95%), N24 for propylene (>99.4%), N35 for isobutane (>99.95%), and N20 for 1-butene (>99.0%), while the purity of nitrogen used as an inert gas during the regeneration procedure was 99.995 mol%.

Fixed Bed Adsorption Apparatus and Procedure

The adsorber bed was a stainless steel column packed with 261 g of 13X zeolite (humid). Fixed bed column properties are listed in Table 2 and a schematic diagram of the experimental setup is presented in Fig. 1. The

Table 2. Characteristics of the fixed bed column

Parameters	Value	Unit
Bed radius R_w	$1.07 \cdot 10^{-2}$	m
Bed length L	0.84	m
Sample mass m	0.250	kg
Bed porosity ε_b	0.39	–
Bulk density ρ_b	820	kg.m^{-3}
Wall density ρ_w	8238	kg.m^{-3}
Feed flowrate Q_0	1.00	slpm*

*SLPM = Standard Liter Per Minute (273 K and 101 kPa).

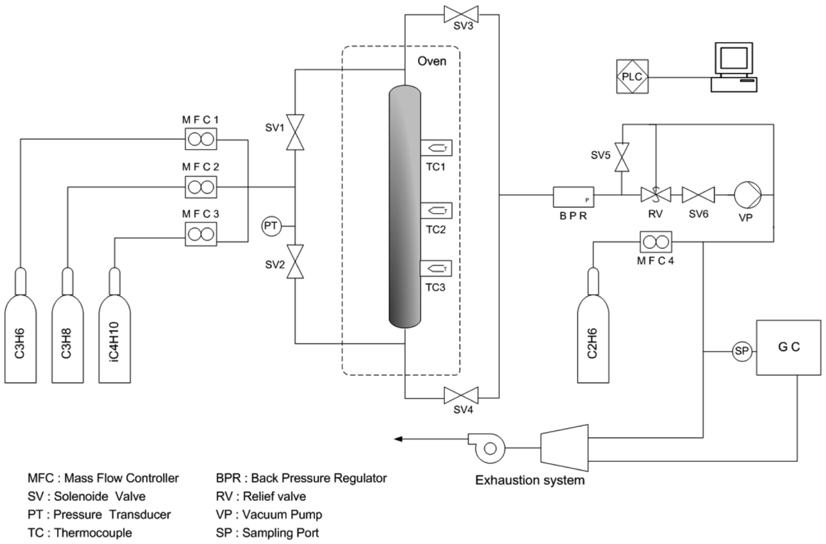

Figure 1. Schematic diagram of the fixed bed adsorption breakthrough apparatus.

column was 2.14 cm in internal diameter by 84 cm high and was vertically oriented to distribute the packing evenly across the column's diameter. The remaining void volume at both ends of the column was filled with glass beads, preventing consequently a too large void volume at the end. The column was then placed inside a convective furnace and three Omega type K thermocouples were mounted at regular intervals down the column's length, about 25 cm apart, measuring the gas temperature profiles at the bottom and the middle of the column while the thermocouple placed at the top, in contact with the column shell, measures the wall column temperature. Feed to the column was supplied by three high pressure storage tanks containing pure propane (C_3H_8), pure propylene (C_3H_6), and either pure isobutane (iC_4H_{10}) or pure 1-butene (C_4H_8), respectively. Note that these gases were used without any further treatment. The flow of each gas was regulated by a mass flow controller (Teledyne, USA) to get a constant flow and an exact mole fraction of each species in the gas phase at the inlet. The gas streams were mixed at the tubing cross, where a backpressure regulator (Bronkhorst, Holland) was also attached. At the column exit, the effluent from the bed (a given binary mixture of hydrocarbons) was analyzed by a Chromopack CP9001 gas chromatograph equipped with a multi-port sampling valve system and a FID detector, using ethane as an external reference flow. The room temperature containing the equipment is maintained under air-conditioning to keep an almost constant ambient temperature of 298 K with a maximum variation of ± 2 K. Before each experiment, the 13X zeolite bed was dehydrated by purging it overnight under a slight flow of nitrogen from ambient temperature to 593 K with a ramp of 2 K·min^{-1}. Binary experiments were performed with a total flowrate of 1.0 SLPM at a constant temperature of 373 K and a pressure of 150 kPa for the following mixtures: C_3H_6-C_3H_8, iC_4H_{10}-C_3H_8, iC_4H_{10}-C_3H_6; and 110 kPa for C_4H_8-C_3H_8 and C_4H_8-C_3H_6 systems.

THEORETICAL SECTION

The ideal adsorbed solution (IAS) theory developed by Myers and Prausnitz (22) provides an effective method to predict adsorption equilibrium of gas mixtures from pure component isotherms. The IAST is a thermodynamically rigorous theory based on the perfect mixing of individual components at constant spreading pressure to form an ideal solution. An important advantage of the IAS theory is that it puts no restrictions on description of adsorption equilibrium of the pure components, i.e., different isotherm models can be used to fit the adsorption equilibrium data of different pure components when IAS theory is used. This is essential to simplify the solution of the spreading pressure because its analytical solution can likely be obtained using the suitable isotherm model or the iterative procedure for its numerical solution can be simplified.

Another attractive way to predict binary adsorption equilibria is to extend a single-component isotherm to multicomponent adsorption models by respecting the thermodynamic principles and the physical structure of the selected adsorbent. Thus the Toth model employed in the previous works (15,16) can be basically extended by means of two approaches; a ready-made model (25) based on thermodynamics and one established according to physical basis, i.e., the 13 X zeolite framework and more exactly the loading capacity of its supercage for a given molecule.

Ideal Adsorbed Solution Theory (IAST)

The ideal adsorbed solution theory developed by Myers and Prausnitz can be used to predict adsorption equilibria of mixture gases on the basis of pure gas isotherms only. The basic equation for IAST can be written as:

$$y_i P = x_i P_i^0(\pi) \tag{1}$$

where y_i and x_i are the gas phase and the adsorbed phase mole fractions for component i, respectively, π is the spreading pressure of the adsorbed phase, and P_i^0 is the hypothetical pressure of a pure component that gives the same spreading pressure than the adsorbed mixture on the surface. The spreading pressure can be calculated by the following equation:

$$\frac{\pi A}{RT} = \int_0^{P_i^0} \frac{q_i^0(P)}{P} dP \tag{2}$$

where $q_i^0(P_i^0)$ is the pure component isotherm and A is the specific surface area.

Assuming that the pure component adsorption isotherms can be fitted by a physically consistent Toth (PCT) model, i.e., with different saturation capacities for each component, the isotherm can be expressed as follows:

$$q_i^0 = q_{m,i} \frac{K_{eq,i} P}{\left(1 + \left(K_{eq,i} P\right)^{\vartheta}\right)^{1/\vartheta_i}}, \text{ and } K_{eq,i} = K_{eq,i,0} \exp\left(\frac{-\Delta H_i}{RT}\right) \tag{3}$$

where q_i^0 is the absolute adsorbed amount of the single component i, $K_{eq,i}$ is the affinity parameter of the pure component i for the solid sorbent, ΔH_i is the isosteric heat of adsorption at zero loading, ϑ_i is the solid heterogeneity parameter and $q_{m,i}$ is the maximum loading capacity of the sorbent. It should be noted however, that the saturation adsorption capacities are commonly forced to be the same for all the species in order to be in accordance with thermodynamics. To distinguish this latter case with a model based on a variable saturation capacity for each component (alias PCT model), the resulting equation will be called thermodynamically consistent Toth model (TCT).

The IAS theory can thereafter be combined either with the PCT or TCT model (in this study the IAST will be combined with the PCT isotherm). So the reduced spreading pressure ω can be calculated from Eqs. (2) and (3), and written in terms of fractional loading θ, as follows:

$$\omega = \frac{\pi A}{RT} = q_{m,i}\left(-\left(\frac{1}{\vartheta} - 1\right)\theta - \frac{\theta^{1/n}\ln(1-\theta)}{\vartheta} - \left(\frac{1}{\vartheta} - 1\right)\sum_{k=1}^{\infty}\frac{\theta^{(1+k\vartheta)}}{(1+k)(1+k\vartheta)}\right) \tag{4}$$

Note that the reduced spreading pressure for each component should be equal at equilibrium. Furthermore, the following mole fractions constraints should be set:

$$\sum_{i=1}^{N} x_i = 1 \quad \text{and} \quad \sum_{i=1}^{N} y_i = 1 \tag{5}$$

Finally, the total amount of adsorbed gases q_i depends on the amount adsorbed in the standard state q_i^0 and can be expressed according to the following relationship:

$$\frac{1}{q_t} = \sum_{i=1}^{N} \frac{x_i}{q_{\mathrm{i}}{}^{0}(P)} \tag{6}$$

It should be mentioned that the set of Eqs. (1)–(6) were resolved by numerical integration at each step of the iteration procedure through a MATLAB program developed by the group of Prof. Do (26).

Extended Toth Model with Thermodynamical Consistency (TCET)

The Toth adsorption isotherm can easily be extended to the multicomponent adsorption system by keeping all the assumptions made in this model for the treatment of pure component adsorption equilibria. By extending this model to multicomponent systems the adsorbed amount of component i can be written as:

$$q_i = q_{\mathrm{m}} \frac{K_{eq,i} P y_i}{\left(1 + \left(\sum_{i=1}^{N} K_{eq,i} P \, y_i\right)^{\vartheta_T}\right)^{1/\vartheta_T}} \quad \text{with } q_m = q_{m,i} = q_{m,j} \tag{7}$$

It is worth noting that the extended Toth equation is used with a global heterogeneity parameter ϑ_T. This parameter is different from the single parameter ϑ_i used in the pure component Toth model. It is calculated from the single component isotherms with:

$$\vartheta_T = \sum_{i=1}^{N} y_i \vartheta_i \tag{8}$$

As mentioned before, the saturation capacities of different species in the thermodynamically consistent extended Toth isotherm (TCET) should be theoretically the same to meet the thermodynamic consistency (27). However, for physical adsorption of molecules of very highly different sizes this constraint becomes implausible (28) and can consequently compromise the predictability of the model.

Extended Toth Model with Physical Consistency (PCET)

In the physically consistent extended Toth model (PCET), the saturation adsorption capacity is on the opposite assumed to be different for each species in order to take into account both the framework specificity of 13X zeolite, i.e., the volume of the "supercage" (29), and the critical diameter of each adsorbate. Applying this physical constraint, the extended Toth model is rewritten as follows:

$$q_i = q_{m,i} \frac{K_{eq,i} P y_i}{\left(1 + \left(\sum_{i=1}^{N} K_{eq,i} P \, y_i\right)^{\vartheta_T}\right)^{1/\vartheta_T}} \quad \text{with } q_{m,i} \neq q_{m,j} \tag{9}$$

As for the previous model, the global parameter ϑ_T defining the degree of the system heterogeneity is assumed to be the same for a given gas mixture on the selected adsorbent (25) in order to satisfy thermodynamic requirements (27). Although a global and unique heterogeneity parameter is required thermodynamically, it is also necessary to set additional restrictions with physical basis in order to avoid meaningless fitting parameters. As a result, it was also assumed that this global parameter simply varies with the feed gas phase composition. To substantiate this equation with respect to the variable saturation capacity, it should be emphasized that the unit cell composition of the commercial 13X zeolite used in this work is $Na_{88}Al_{88}Si_{104}O_{384}$ whose structure is made up of 15 Å diameter supercages. Thus, in view of the adsorbates molecular diameter reported in Table 3, it stands to reason that the number (integer) of molecules of widely different size and geometry cannot be the same inside a given supercage at saturation. Therefore, for volume filling considerations it is easily realized that the adsorption capacity on 13X zeolite should be a function of the molecular size. In addition, all molecular simulation studies performed on adsorption of diverse hydrocarbons over faujasite type zeolites (32–34), have highlighted a variable saturation amount of each species in terms of molecules per cage or molecule per unit cell.

Table 3. Characteristics diameters of the adsorbates

Adsorbate	σ (Å)
Propane	3.9 (30)
Propylene	3.1 (30)
Isobutane	5.0 (31)
1-Butene	4.5 (31)

RESULTS AND DISCUSSION

Single Gas Adsorption Isotherms

The measurements of single component adsorption isotherms were conducted using a gravimetric technique whose detailed results were reported in previous papers (15,16). In Fig. 2a are presented the single component adsorption isotherms of propane, propylene, isobutane and 1-butene on 13X zeolite at 373 K. As seen in this figure all pure component isotherms can be classified as Type I according to the classification of Brunauer et al., (35). Therefore the experimental data can be successfully correlated by the two types of Toth isotherm (i.e., physically or thermodynamically consistent). The fitted parameters obtained with both models are tabulated in Table 4. As expected in the case of the PCT model, the saturated amounts adsorbed for the studied species are markedly different. For instance, the extracted saturation capacity for 1-butene is higher than for isobutane. This difference in the saturation can be explained by the molecular diameter of 1-butene (0.45 nm) which is smaller than that of isobutane (0.50 nm). Although all molecules can access the supercage of the zeolite through 7.4 Å diameter windows, the number of isobutane molecules per cage must be less than that of 1-butene. The values of the adsorption enthalpy ΔH_i at zero coverage for each species are also presented in Table 4. For both models the highest value of adsorption enthalpy was found for 1-butene. It indicates that there is a stronger

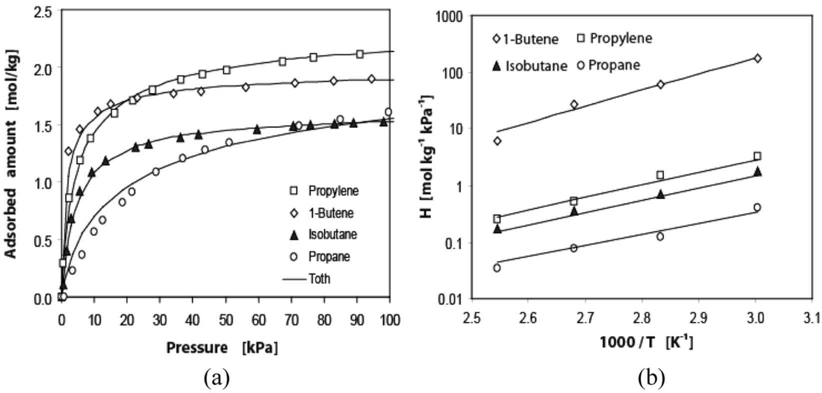

(a) (b)

Figure 2. (a) Single adsorption isotherms of propane, propylene, isobutane and 1-butene on 13X zeolite at 373 K (Lines are the PCT model fits); (b) Arrhenius plot of Henry constant values obtained from the PCT model and from experimental adsorption isotherms (15,16).

Table 4. Optimal values of fitted adsorption parameters in PCT and TCT models

Gas	PCT (15,16) $q_{m,i} \neq q_{m,j}$	TCT $q_{m,i} = q_{m,j}$
Propane		
$q_{m,i}$ (mol/kg)	2.20	2.30
$-\Delta H_i$ (kJ/mol)	36.9	38.5
$b_{i,0}$ (10^{-7}kPa^{-1})	2.5	3.5
θ_i (–)	0.892	0.685
Propylene		
$q_{m,i}$ (mol/kg)	2.59	2.30
$-\Delta H_i$ (kJ/mol)	42.4	43.6
$b_{i,0}$ (10^{-7}kPa^{-1})	2.5	3.5
θ_i (–)	0.658	0.620
Isobutane		
$q_{m,i}$ (mol/kg)	1.78	2.30
$-\Delta H_i$ (kJ/mol)	41.6	41.1
$b_{i,0}$ (10^{-7}kPa^{-1})	2.5	3.5
θ_i (–)	0.848	0.528
1-Butene		
$q_{m,i}$ (mol/kg)	2.10	2.30
$-\Delta H_i$ (kJ/mol)	54.4	51.2
$b_{i,0}$ (10^{-7}kPa^{-1})	2.5	1.5
θ_i (–)	0.452	0.515

interaction between the adsorbate and the adsorbent for 1-butene on 13X zeolite whatsoever the model employed.

Through the pure-component isotherms, it is worth evaluating the Henry's constant in order to discuss the adsorption affinity before measuring binary adsorption data. Thus, by using both experimental (symbols) and PCT isotherms (lines), the Henry's constant were calculated for different temperatures (see Table 5) and plotted in Fig. 2b as a function of inverse temperature. Although the calculated Henry's constants were extrapolations based on the isotherms used, this figure allows nevertheless making out the following selectivity sequence: 1-butene >propylene > isobutane > propane. It is worth pointing out that 1-butene has indeed the highest Henry's law constant among the adsorbates studied which implies a strong affinity of the 13X zeolite for 1-butene. Additionally, it should be noted that the linearity of these plots, indicates that meaningful thermodynamic parameters can be extracted from the PCT model.

Table 5. Henry's law constants for 13X zeolite at four different temperatures*

Adsorbate	$H_{333\,K}$ (mol.kg^{-1}. kPa^{-1})	$H_{353\,K}$ (mol.kg^{-1}. kPa^{-1})	$H_{373\,K}$ (mol.kg^{-1}. kPa^{-1})	$H_{393\,K}$ (mol.kg^{-1}. kPa^{-1})
Propane	0.337	0.158	0.0809	0.0441
Propylene	2.899	1.218	0.561	0.279
Isobutane	1.492	0.637	0.298	0.151
1-Butene	182	59.92	22.16	9.068

Note: The related experimental adsorption isotherms are reported in previous works (15,16).

Binary Breakthrough Curves

In Fig. 3 are shown typical breakthrough curves of three hydrocarbon mixtures, namely propylene/propane, propylene/isobutane, and propylene/1-butene at 373 K with the related temperature histories at the bottom, middle, and top of the column. Note that for propylene/desorbent mixtures, the adsorbent bed was initially saturated with propane in order to be close to the simulated moving bed operation conditions. Figure 3a shows the breakthrough profiles of a binary mixture of propylene and propane (50:50) on 13X zeolite, with a typical roll-up indicating a displacement of adsorbed propane by propylene. According to the equilibrium theory, this result was expected due to the favorable nature of the pure propylene adsorption isotherm. The breakthrough profiles of propylene/isobutane mixture (50:50) presented in Fig. 3b, also exhibit a roll-up which indicates once again that 13X zeolite selectively adsorbs the propylene. However, it is seen in Fig. 3c that 1-butene is this time-preferentially adsorbed during the adsorption of propylene/1-butene mixture (50:50) through a fixed bed adsorbent initially saturated with propane. As stated previously via the Van't Hoff plot of Henry's constant, the adsorption isotherm of 1-butene is highly favorable compared to the ones of the C_3 components.

Based on these breakthrough curves, the adsorbed amount at equilibrium, q_i for each component of a given mixture was calculated by the following mass balance:

$$q_i = \frac{1}{\rho_p(1-\varepsilon_b)V_c}\int_0^{\infty}(F_0 - F_1)dt - \frac{\varepsilon_b}{\rho_p(1-\varepsilon_b)}\frac{F_0}{Q_0} \tag{10}$$

where ρ_p is the pellet density, ε_b is the bed void fraction, V_c is the volume of the column occupied by the solid adsorbent, Q_0 is the feed volumetric

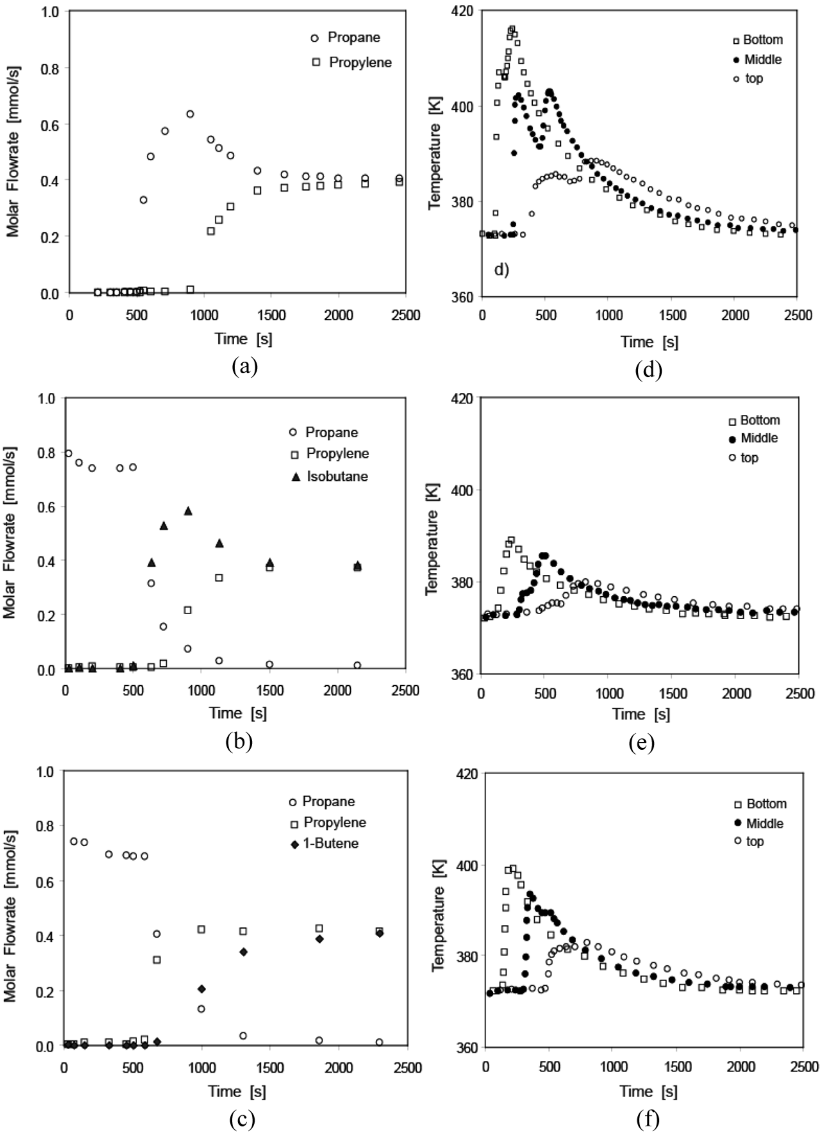

(a) (d)

(b) (e)

(c) (f)

Figure 3. Experimental multicomponent breakthrough curves on 13X zeolite at 373 K. (a) Breakthrough curves of propylene/propane mixture (50:50) at 150 kPa. (b) Breakthrough curves of propylene/isobutane mixture (50:50) over an adsorbent bed initially saturated with propane at 150 kPa. (c) Breakthrough curves of propylene/1-butene mixture (50:50) over an adsorbent bed initially saturated with propane at 110 kPa. (d), (e) and (f) represent the related temperature histories at the bottom, middle and top of the column, respectively.

flowrate, and F_0 is the feed molar flowrate. The evolution of F_i at the bed exit is taken into account in the calculation, which was measured experimentally. Besides the calculation of the adsorbed amounts, it is common and useful to determine the selectivity in order to highlight the affinity of an adsorbent for a given species. The selectivity is usually defined as fellows:

$$\alpha_{12} = \frac{x_1/y_1}{x_2/y_2} \tag{11}$$

where x is the mole fraction in the adsorbed phase and y is the mole fraction in the gas phase. The experimental binary adsorption data and the related selectivities are listed in Table 6. It is worth pointing out that the data listed in this table were obtained through breakthrough curves analogous to the ones presented in Figure 3 and following the same methodology.

Binary Adsorption Equilibria

Predictions of binary adsorption equilibrium from single component isotherm were examined by using IAST, TCET, and PCET models and compared to the experimental data tabulated in Table 6. As stated before, the model prediction accuracies are found to be dependent on the accuracy of the pure component isotherm data fitting. In all the binary adsorption graphs, the total and partial amounts adsorbed by each component are plotted versus the mole fraction of a given species in the gas phase. Beyond the loading diagram, a McCabe-Thiele diagram (also known as x-y diagram) is necessary to clearly point out the appropriateness of the selected desorbents, which connects the adsorbed phase mole fraction x_i, with the gas phase mole fraction y_i of the key component.

Coadsorption of Propylene and Propane

Figure 4 shows the adsorption experimental data (symbols) of propylene-propane mixture on 13X zeolite, along with the predictions from the three models studied (lines). It is seen from this figure that Propylene (component 1) is more strongly adsorbed over propane (component 2) on 13X zeolite. This is in accordance with the observations made from the binary breakthrough curves and the Henry's law constants. Moreover, the experimental adsorbed amounts found for this system are in good agreement with the ones reported in the literature (36–38). Regarding the models predictions, it can be seen that IAST and PCET models predict the data reasonably well justifying a priori the

Table 6. Binary adsorption isotherms on 13X zeolite at 373 K and 150 kPa (110 kPa for mixtures comprising 1-butene)

Systems	$Y_1(-)$	q_1(mol/kg)	q_2(mol/kg)	$x_1(-)$	$x_2(-)$	$\alpha_{12}(-)$
Propylene (1)	0.00	0.000	1.828	0.000	1.000	–
Propane (2)	0.10	0.592	1.288	0.315	0.685	4.136
	0.25	1.252	0.777	0.617	0.383	4.832
	0.50	1.784	0.333	0.843	0.157	5.364
	0.75	2.046	0.126	0.942	0.058	5.419
	0.90	2.185	0.044	0.980	0.020	5.456
	1.00	2.290	0.000	1.000	0.000	–
Isobutane (1)	0.00	0.000	1.825	0.000	1.000	–
Propane (2)	0.10	0.399	1.309	0.234	0.766	2.743
	0.25	0.810	0.886	0.477	0.523	2.741
	0.50	1.330	0.493	0.730	0.270	2.699
	0.75	1.524	0.201	0.883	0.117	2.524
	0.90	1.586	0.102	0.939	0.061	1.720
	1.00	1.640	0.000	1.000	0.000	–
Isobutane (1)	0.00	0.000	2.290	0.000	1.000	–
Propylene (2)	0.10	0.098	2.133	0.044	0.956	0.414
	0.25	0.244	1.926	0.113	0.887	0.380
	0.50	0.597	1.478	0.288	0.712	0.404
	0.75	1.119	0.900	0.554	0.446	0.415
	0.90	1.382	0.332	0.806	0.194	0.463
	1.00	1.644	0.000	1.000	0.000	–
1-Butene (1)	0.00	0.000	1.622	0.000	1.000	–
Propane (2)	0.25	1.594	0.247	0.866	0.134	19.335
	0.50	1.766	0.127	0.933	0.067	13.910
	0.75	1.856	0.082	0.958	0.042	7.519
	1.00	1.956	0.000	1.000	0.000	–
1-Butene (1)	0.00	0.000	2.076	0.000	1.000	–
Propylene (2)	0.50	1.612	0.472	0.773	0.227	3.413
	1.00	1.948	0.000	1.000	0.000	–

predictability of these two models. Conversely, it is significant that the TCET model performs rather poorly for this mixture. This can be attributed to the fact that the saturation capacity q_m set in this model is the same for both adsorbates even if the critical diameters of these two molecules are quite different (see *Table 3*).

Co-adsorption of Isobutane and Propane

The binary adsorption equilibria of isobutane and propane at 373 K and 150 kPa are shown in Figure 5. Owing to the fact that the adsorption

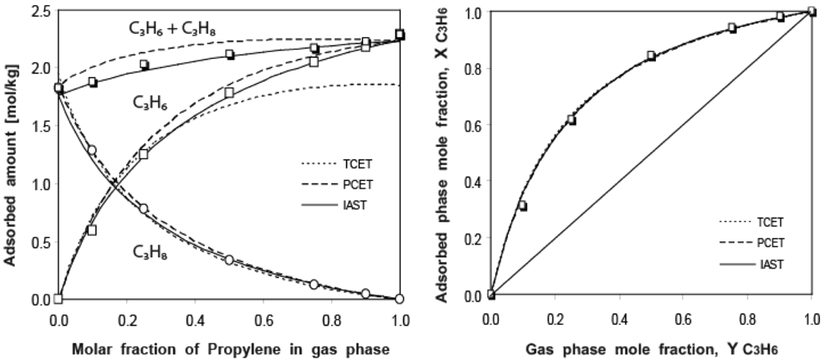

(a) (b)

Figure 4. Models predictions and experimental adsorption equilibrium data of the *propylene-propane* mixture on 13X zeolite at 373 K and 150 kPa. (a) loading diagram; (b) X-Y diagram

isotherm of isobutane is slightly more favorable than that of propane, it logically leads to a preferential adsorption of isobutane as it is noticeably shown in the *x-y* diagram presented in Fig. 5b. Regarding the modeling, it can be seen that all the models predictions seem to be rather good for this system. Nevertheless, in this particular case, although propane is the more weakly adsorbed species, its equilibrated amount adsorbed is of the same order as that of isobutane, the more strongly adsorbed component. As a result, the models prediction for both species should be

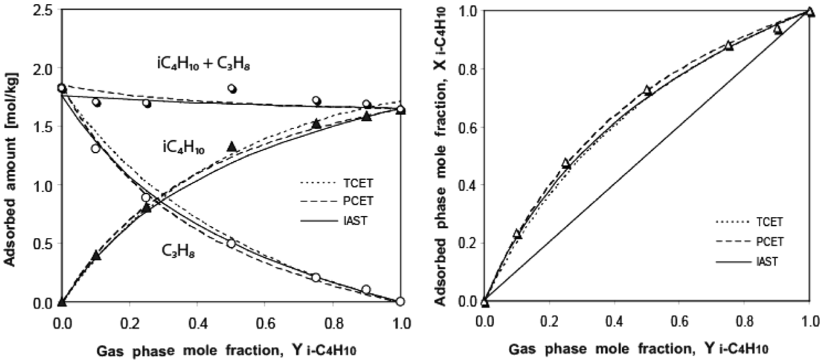

(a) (b)

Figure 5. Models predictions and experimental adsorption equilibrium data of the *isobutane-propane* mixture on 13X zeolite at 373 K and 150 kPa. (a) loading diagram; (b) X-Y diagram

preferentially taken quantitatively. Therefore, to further discriminate the models performance, it is then valuable to describe the disparity between the experimental data and the predicted results by calculating the average relative error (ARE), which is defined as:

$$ARE\ \% = \frac{1}{N_{exp}} \sum_{k=1}^{N} \frac{|q_{cal,k} - q_{exp,k}|}{q_{exp,k}} \times 100 \tag{12}$$

where N_{exp} is the number of experimental points, $q_{cal,k}$ and $q_{exp,k}$ are predicted and experimental values, respectively. The ARE of the models predictions for each case is given in Table 7. Thus, if we pay attention to the results reported in this table, it clearly appears that the adsorbed amount predicted by the PCET model are slightly more accurate (within ±5%) than those obtained from the TCET model (7.62%).

Coadsorption of Isobutane and Propylene

The adsorption behavior of the isobutane-propylene mixture on 13X zeolite at 373 K and 150 kPa is presented in Fig. 6. As noticed previously from the single adsorption isotherms and the breakthrough curves, propylene is preferentially adsorbed over isobutane. This selective adsorption of propylene is also clearly shown through the selectivity values calculated from Eq. (11) and reported in Table 6. With regard to the modeling predictions, the total mixture loading predicted by the IAST model compares very well with the experimental data. On the other hand, the TCET model underpredicts once again propylene adsorption whereas the PCET model predicts the experimental data reasonably well. In addition, the adsorption equilibrium of this mixture on 13X zeolite were also investigated by Granato et al. (34) using *configurational-bias Monte Carlo*

Table 7. Average relative error of the results predicted by IAST, TCET, and PCET models for binary adsorption equilibria on 13X zeolite

			ARE %		
Systems	T (K)	P (kPa)	IAST	TCET	PCET
C_3H_6–C_3H_8	373	150	3.34	8.09	5.43
iC_4H_{10}–C_3H_8	373	150	5.32	7.62	5.36
iC_4H_{10}–C_3H_6	373	150	4.17	9.08	3.27
C_4H_8–C_3H_8	373	110	6.22	13.83	5.96
C_4H_8–C_3H_6	373	110	4.25	11.52	5.88

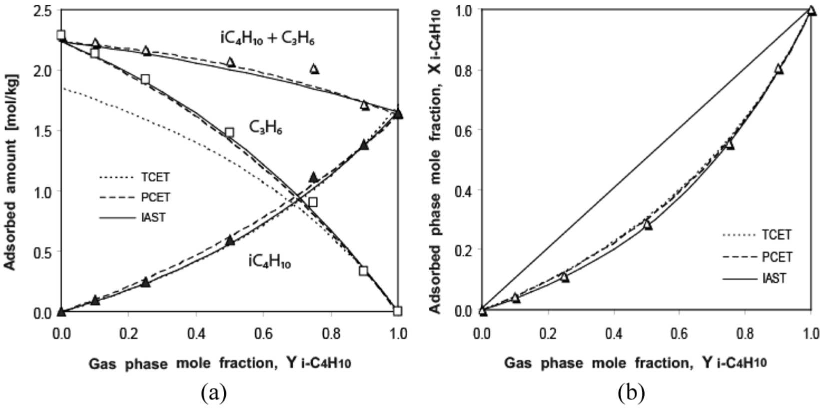

Figure 6. Models predictions and experimental adsorption equilibrium data of the *isobutane-propylene* mixture on 13X zeolite at 373 K and 150 kPa. (a) loading diagram; (b) X-Y diagram

(CBMC) simulations and it appeared that the predicted results agreed well with both the experimental data and the results of the PCET model. To get back to the TCET model, the large ARE found for this model in the isobutane-propylene mixture, and previously in the propylene-propane system, may point out the deficiency of this model in terms of physical consistency.

Desorbent Choice: Isobutane vs 1-Butene

The binary interaction of 1-butene with propane and propylene on 13X zeolite was also investigated experimentally in order to compare its adsorption behavior with the one of isobutane in the presence of C_3 hydrocarbons. The binary adsorption equilibria of both 1-butene/propane and 1-butene/propylene mixtures at 373 K and 110 kPa are presented in a *x*-*y* diagram as function of 1-butene in the gas phase (Fig. 7a). It can be seen from this figure that 1-butene is more selectively adsorbed than propylene as observed before through the Van't Hoff plot of the Henry's law constants. As well, considering the selectivity factors listed in Table 6, it is clearly shown that 1-butene is always preferentially adsorbed over both propane and propylene. Regarding isobutane adsorption behavior in mixture with propane and propylene, respectively, it is observed in Fig. 7b that the adsorption equilibrium of isobutane is perfectly intermediate to the ones of propane and propylene. It should be noticed that this result was expected since the Henry's law constant

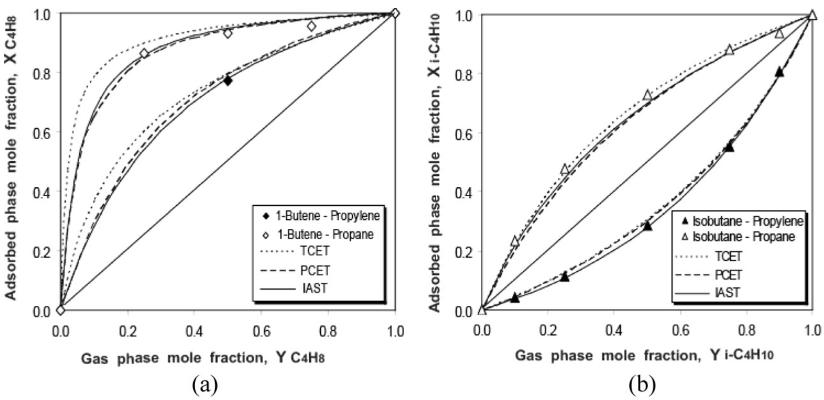

Figure 7. Comparison of 1-butene and isobutane adsorption behavior in mixture with propane and propylene on 13X zeolite at 373 K. (a) X-Y diagram for propane/1-butene and propylene/1-butene at 110 kPa; (b) X-Y diagram for propane/isobutane and propylene/isobutane at 150 kPa

of isobutane was indeed between the values reported for propane and propylene. The *x*-*y* diagram although commonly used to display binary adsorption behavior, does not have enough sensitivity to discriminate between data and models at the accuracy levels necessary for plant design (39). The selectivity is a much more sensitive indicator of adsorption behavior, as illustrated in Fig. 8. It can thus be observed from this selectivity diagram, that isobutane represents de facto an interesting desorbent since it will allow on the one hand the displacement of propane, propylene, and their mixture from the adsorbent bed, and on the other hand will be itself fairly easily removed from the 13X zeolite by adsorption of the C_3 hydrocarbons.

Comments on the Models Predictability

Although the PCET model is not based on rigorous thermodynamic principles (due to the variable saturation capacities) it seems moreover responding favorably to the thermodynamic consistency test pointed by Talu and Myers (40):

1. At fixed temperature and pressure, the total amount adsorbed should correspond to the pure-component values at the composition end points. As Fig. 4 indicates, this test is entirely satisfied.
2. At fixed temperature and pressure, the *x*-*y* diagrams and loading curves of all thermodynamically consistent models must cross the

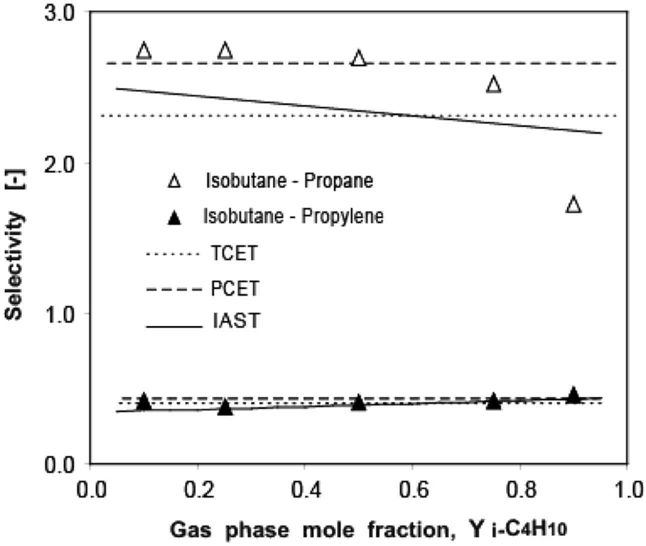

Figure 8. Experimental and models predictions of the selectivities for both isobutane-propane and isobutane-propylene systems on 13X zeolite at 373 K and 150 kPa.

experimental curves at least once in the region of $0 < x < 1$ (this test is generally known as intersection rule (41)). As it is seen in both Fig. 5 and Fig. 6 this test is satisfied.

3. The selectivity must approach the value determined by the Henry's law constants at zero pressure and reported in Table 5. From the Fig. 8, it is clearly seen that this test is also satisfied.

Figure 9 shows the comparison between the adsorbed phase mole fraction predicted by the PCET model and the experimental data. As seen in this figure the model was found to describe the experimental data of all the studied hydrocarbon mixtures with a reasonably good accuracy. Concerning the IAST performance, Valenzuela and Myers (42) have already reported that the predictions resulting from the IAST are thermodynamically rigorous and completely independent of the particular equation adopted for the pure component isotherms. The comparison between the IAST and PCET models shows that the predictions from the two models are very close (see Table 7). This implies that the prediction ability of the IAS theory and the PCET model is similar in the current adsorption systems investigated. However, since the IAS model is computationally complex, its use will require considerable CPU time

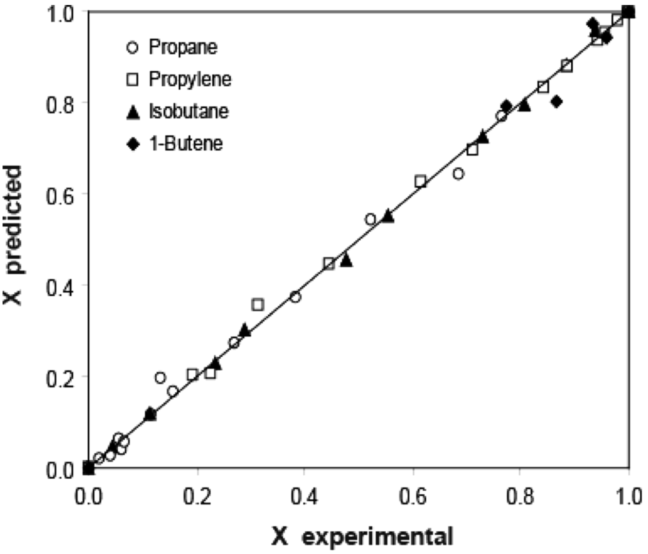

Figure 9. Comparison of the experimental adsorbed phase mole fraction with the PCET predictions for all hydrocarbon mixtures.

in modelling SMB dynamics. Finally, considering the lack of physical meaning of a fixed saturation adsorbed amount, the validity of the TCET model is limited to adsorptive molecules within a certain range of molecular size.

CONCLUSION

The binary adsorption equilibria of several hydrocarbons mixtures, namely propylene-propane, isobutane-propane, isobutane-propylene, 1-butene-propane, and 1-butene-propylene were measured on 13X zeolite using a dynamic method through fixed bed adsorption experiments. It was found that the TCET model performs rather poorly for the studied mixtures due to some meaningless physical parameters. On the other hand, the PCET model predicts with acceptable accuracy the binary adsorption data and can easily be integrated in a general dynamic simulation of a SMB process over the entire conditions of design interest. Although the IAST model can predict the experimental data with a better accuracy, the PCET model seems to be suitable due to its simple analytical resolution, which will allow a significant reduction of the computation time needed for repeated solution of simultaneous design equation describing the mass, momentum, and energy balances for the propane-propylene separation by SMB process.

ACKNOWLEDGMENTS

The authors acknowledge financial support from the Institut Français du Pétrole (IFP). N.L. gratefully acknowledges the grant from Association Nationale de la Recherche Technique (Research fellowship: CIFRE 518/2004). MAG thanks financial support from Fundação para a Ciência e a Tecnologia (FCT) through grant BD-16449/2004. PSG also acknowledges FCT through grant BD-22103/2005.

NOTATION

A	specific surface area (m^2/kg)
F_i	molar flowrate of component i (mmol/s)
H_i	Henry's law constant for component i (mol/ kg.kPa)
ΔH_i	isosteric heat of adsorption of component i (J/mol)
$K_{eq,i}$	adsorption equilibrium constant (–)
L	length of the column (m)
M	molecular weight (g/mol)
P	gas pressure (kPa)
Q	volumetric flowrate (SLPM)
q_i	adsorbed amount of component i (mol/kg)
q_m	maximum loading capacity of the sorbent (mol/kg)
R	ideal gas constant ($= 8.3143$ J/ mol.K)
r_c	crystal radius (m)
r_p	pore radius (m)
R_p	pellet radius (m)
t	time variable (s)
T	temperature (K)
x_i	mole fraction of component i in the adsorbed phase (–)
y_i	mole fraction of component i in the gas phase (–)

Greek Letters

ε_b	bulk porosity (–)
ε_p	pellet porosity (–)
α	selectivity (–)
ρ_p	pellet density (kg/m^3)
θ	heterogeneity of the solid adsorbent -Toth parameter (–)

π	spreading pressure (N/m)
ω	reduced spreading pressure (mol/kg)

Abbreviations

CBMC	Configurational-bias Monte Carlo
PCET	Physically Consistent Extended Toth model
PCT	Physically Consistent Toth model
PSA	Pressure Swing Adsorption
SMB	Simulated Moving Bed
TCET	Thermodynamically Consistent Extended Toth model
TCT	Thermodynamically Consistent Toth model

REFERENCES

1. Manley, D.B.; Swift, G.W. (1971) Relative volatility of propane-propene system by integration of general coexistence equation. *J. Chem. Eng. Data*, *16* (3): 301.
2. Eldridge, R.B. (1993) Olefin/paraffin separation technology: a review. *Ind. Eng. Chem. Res.*, *32* (10): 2208.
3. Bryan, P.F. (2004) Removal of propylene from fuel-grade propane. *Sep. Pur. Rev.*, *33* (2): 157.
4. Eldridge, R.B.; Siebert, F.A.; Robinson, S. (2005) Hybrid separations/distillation technology. *Research opportunities for energy and emissions reduction*. (http://www1.eere.energy.gov/industry/chemicals).
5. Ghosh, T.K.; Lin, H.-D.; Hines, A.L. (1993) Hybrid adsorption-distillation process for separating propane and propylene. *Ind. Eng. Chem. Res.*, *32* (10): 2390.
6. Kumar, R.; Golden, T.C.; White, T.R.; Rokicki, A. (1992) Novel adsorption distillation hybrid scheme for propane/propylene separation. *Sep. Sci. Tech.*, *27* (15): 2157.
7. Ruthven, D.M.; Farooq, S.; Knaebel, K.S. (1994) *Pressure Swing Adsorption*; VCH Publishers: New York, USA.
8. Da Silva, F.A.; Rodrigues, A.E. (2001) Propylene/propane separation by VSA using 13X zeolite. *AIChE J.*, *47* (2): 341.
9. Da Silva, F.A.; Rodrigues, A.E. (2001) Vacuum swing adsorption for propylene/propane separation with 4A zeolite pellets. *Ind. Eng. Chem. Res.*, *40* (24): 5758.
10. Rege, S.U.; Yang, R.T. (2002) Propylene/propane separation by PSA: sorbent comparison and multiplicity of cyclic steady states. *Chem. Eng. Sci.*, *57* (7): 1139.
11. Grande, C.A.; Rodrigues, A.E. (2005) Propane/propylene separation by pressure swing adsorption using zeolite 4A. *Ind. Eng. Chem. Res.* *44* (23): 8815.
12. Rodrigues, A.E.; Lamia, N.; Grande, C.A.; Wolff, L.; Leflaive, P.; Leinekugel-le-Cocq, D. Procédé de Séparation du Propylène en Mélange avec du Propane par Adsorption en Lit Mobile Simulé en Phase Gaz ou Liquide

utilisant une Zéolithe de type Faujasite 13X comme Solide Adsorbant. FR. Patent 2.903.981, July, 2006; Int. Patent WO.2008.012410, January, 2008.

13. Broughton, D.B.; Gerhold, C.G. (1961) Continuous Sorption Process Employing Fixed bed of Sorbent and Moving Inlets and Outlets. U.S. Patent. 2: 985,589.
14. Ruthven, D.M.; Ching, C.B. (1989) Countercurrent and simulated countercurrent adsorption separation processes. *Chem. Eng. Sci.*, *44* (5):1011.
15. Lamia, N.; Wolff, L.; Leflaive, P.; Sà Gomes, P.; Grande, C.A.; Rodrigues, A.E. (2007) Propane/Propylene separation by simulated moving bed I. Adsorption of propane, propylene and isobutane in pellets of 13X zeolite. *Sep. Sci. Tech.*, *42* (12): 2539.
16. Lamia, N.; Wolff, L.; Leflaive, P.; Leinekugel-le-Cocq, D.; Sà Gomes, P.; Grande, C.A.; Rodrigues, A.E. (2008) Equilibrium and fixed bed adsorption of 1-butene, propylene and propane over 13X zeolite pellets. *Sep. Sci. Tech.* *43* (5): 1124.
17. Sircar, S. (2006) Basic research needs for design of adsorptive gas separation processes. *Ind. Eng. Chem. Res.* *45* (16): 5435.
18. Nicoud, R.M.; Bailly, M.; Kinkel, J.N.; Devant, R.; Hampe, T.; Kiisters, E. (1993) *Simulated Moving Bed: Basics and Applications*. Nicoud, R.M. (Editor), INPL: Nancy, France.
19. Sircar, S. (2007) Recent developments in macroscopic measurement of multicomponent gas adsorption equilibria, kinetics, and heats. *Ind. Eng. Chem. Res.* *46* (10): 2917.
20. Buss, E. (1995) Gravimetric measurement of binary gas adsorption equilibria of methane-carbon dioxide mixtures on activated carbon. *Gas Sep. Purif*, *9*: 189.
21. Keller, J.U.; Dreisbach, F.; Rave, H.; Staudt, R.; Tomalla, M. (1999) Measurement of gas mixture adsorption equilibria of natural gas compounds on microporous sorbents. *Adsorption*, *5* (3): 199.
22. Myers, A.L.; Prausnitz, J.M. (1965) Thermodynamics of mixed-gas adsorption. *AIChE J.*, *11*: 121.
23. Kapoor, A.; Ritter, J.A.; Yang, R.T. (1990) An extended Langmuir model for adsorption of gas mixtures on heterogeneous surfaces. *Langmuir*. *6* (3): 660.
24. Tóth, J. (1971) State equations of the solid-gas interface layers. *Acad. Sci. Hung.* *69* (3): 311.
25. Jaroniec, M.; Tóth, J. (1976) Adsorption of gas mixtures on heterogeneous solid surfaces: I. Extension of Tóth isotherm on adsorption from gas mixtures. *Colloid and Polymer Science*, *254* (7): 643.
26. Do, D.D. (1998) *Adsorption Analysis: Equilibria and Kinetics*, Series on Chemical Engineering; Imperial College Press: London, U.K.
27. Rao, M.B.; Sircar, S. (1999) Thermodynamic consistency for binary gas adsorption equilibria. *Langmuir*. *15* (21): 7258.
28. Ruthven, D.M. (1984) *Principles of Adsorption and Adsorption Processes*, John Wiley and Sons Inc.: New York, USA.
29. Olson, D.H. (1995) Crystal structure of dehydrated NaX. *Zeolites*, *15* (5): 439.

30. Johnson, J.; Gembicki, S. (2007) The role of adsorption in meeting future energy challenges. *9th Int. Conf. on Fundamentals of Adsorption*–FOA9, Sicily.
31. Breck, D.W. (1974) *Zeolite Molecular Sieves*, John Wiley and Sons Inc.: New York, USA.
32. Granato, M.A.; Vlugt, T.J.H.; Rodrigues, A.E. (2007) Molecular simulation of propane-propylene binary adsorption equilibrium in zeolite 13X. *Ind. Eng. Chem. Res.*, *46* (22): 7239.
33. Zhang, Y.; Furukawa, S.-I.; Nitta, T. (2004) Monte Carlo simulation studies on adsorption of propane/propylene in NaX zeolite. *J. Chem. Eng. Jpn. 37* (4): 563.
34. Granato, M.A; Lamia, N.; Vlugt, T.J.H.; Rodrigues, A.E. (2008) Adsorption equilibrium of isobutane and 1-butene in zeolite 13X by molecular simulation. *Ind. Eng. Chem. Res. 47* (16): 6166.
35. Brunauer, S.; Deming, L.; Deming, W.E.; Teller, E. (1940) On a theory of the van der Waals adsorption of gases. *J. Am. Chem. Soc. 62* (7): 1723.
36. Costa, E.; Calleja, G.; Jimenez, A.; Pau, J. (1991) Adsorption equilibrium of ethylene, propane, propylene, CO_2 and their mixtures on 13X zeolite. *J. Chem. Eng. Data*, *36* (2): 218.
37. Huang, Y.-H.; Johnson, J.W.; Liapis, A.I.; Crosser, O.K. (1994) Experimental determination of binary equilibrium adsorption and desorption of propane-propylene mixtures on 13X molecular sieves by a differential sorption bed system and investigation of their equilibrium expressions. *Sep. Tech.*, *4* (3): 156.
38. Van Miltenburg, A.; Gascon, J.; Zhu, W.; Kapteijn, F.; Moulijn, J.A. (2008) Propylene/propane mixture adsorption on faujasite sorbents. *Adsorption*, *14* (3): 309.
39. Sircar, S. (1996) R&D Note: data representation for binary and multicomponent gas adsorption equilibria. *Adsorption*, *2* (4): 327.
40. Talu, O.; Myers, A.L. (1988) Rigorous thermodynamic treatment of gas adsorption. *AIChE. 34* (11): 1887.
41. Myers, A.L. (1987) *Fundamentals of Adsorptions*, A.I. Liapis, Engineering Found: New York, USA.
42. Valenzuela, D.P. andMyers, A.L. (1989) *Adsorption Equilibrium Data Handbooks*, Prentice-Hall: USA.